13th Australasian Fluid Mechanics Conference
Monash University, Melbourne, Australia
13-18 December 1998

Steady Convective Exchange Flows Down Slopes - Field and Laboratory Experiments

J. J. Sturman, C. E. Oldham, and G. N. Ivey

Centre for Water Research and Department of Environmental Engineering,
University of Western Australia, Nedlands, Western Australia,
AUSTRALIA

ABSTRACT

Horizontal exchange flows driven by destabilising surface buoyancy fluxes due to cooling are important in contributing to the transport of nutrients, micro-organisms and pollutants from littoral to pelagic zones in lakes and the coastal ocean. In particular we are interested in the magnitude of the discharge down a sloping bottom caused by destabilizing forcing fluxes. We develop scaling arguments to predict the dependency of this discharge upon the strength of surface forcing and the angle of the slope. From the discharge and the slope geometry we also predict the flushing timescale of the wedge. The predicted discharge rate agrees well with laboratory, field and numerical measurements covering a wide range of parameters.

INTRODUCTION

This work is motivated by an interest in convectively driven horizontal exchange flows in the side arms and shallow littoral regions of lakes, semi-enclosed seas and coastal ocean environments. We deal mainly with the steady state condition of flows driven by buoyancy fluxes through the water surface overlying a sloping bottom, although unsteady forcing can be an important feature of the field situations (eg. Sturman & Ivey 1998 - SI in future). Considerable insight has already been obtained into flows down bottom slopes in the laboratory (eg. Horsch 1988a,b) in sidearms of reservoirs (Monismith, Imberger & Morison 1990, James & Barko 1991) and by the use of numerical modelling (Horsch, Stefan & Gavali, 1994) and the use of both numerical modelling and analytical techniques (Farrow & Patterson 1993, laminar flow). These earlier studies still leave unanswered such fundamental questions as: how is the mean or 'steady state' discharge down the slope dependent upon the buoyancy flux and slope, and when is it reached? We address these questions by undertaking field and laboratory studies as well as drawing upon data from the published literature.

FIELD METHODS AND RESULTS

Our field measurements were undertaken in Lake Yangebup (South of Perth) which is a small shallow lake sloping relatively steeply from the shoreline and terminating in a relatively flat interior. Preliminary investigations undertaken by the authors in the lake showed that a convective circulation could be clearly identified on days with low wind when there was high insolation in the day followed by clear skies at night with significant night-time cooling fluxes. Therefore our field experiments were conducted in the (Southern) spring, when such conditions were common. Vertical velocity profiles were taken with a SONTEK™ acoustic doppler velocity probe and temperatures were taken from thermistor chains at a site near the base of the slope from the shore. In addition wind speed and direction and solar radiation measurements were taken on site. Figure 1 shows a 'perspective' velocity profile of the resultant of the two horizontal velocity components at this station during a period of low wind, demonstrating a shoreward surface flow and a downslope bottom flow deriving from destabilizing surface forcing which started about 14 hours earlier. From such profiles discharges can be derived for comparison with the scaling results, and a typical discharge in Lake Yangebup is compared with laboratory results below. In general we found that there were significant flows associated with thermal forcing through the water surface when winds were minimal and there were also substantial phase lags between the thermal forcing and the flow responses. Thus interpretation of the data was not easy without knowing the timescale to establish such flows and their spatial form, and this motivated our laboratory experimental programme.

LABORATORY METHODS AND RESULTS

In response to the complexities of the field data, we undertook laboratory studies in a modified version of the facility described in detail in SI. The facility consisted essentially of a

long rectangular box with a horizontal cooling plate on the upper surface of one end and a horizontal heating plate on the lower surface at the other end. Thus we operated two sided experiments and the configuration gave rise to destabilising forcing at the ends, constant bulk tank temperature and minimal heat losses from the tank. Sloping bottoms were installed opposite the forcing plates, corresponding exactly with them in horizontal dimension, thereby modelling surface cooling over sloping bottoms in the field.

Flow visualisation and velocity measurements were made. Figure 2 shows an image of a flow down a slope in response to cooling at close to steady state. The image was obtained by seeding the flow with fluorescent particles of about 45-120μm diameter and illuminating the flow near the tank centreline with a vertical sheet of laser light from an argon ion laser. There is a turbulent boundary layer beneath the forcing plate with flow in the left hand direction. Individual thermals are evident below 'H'. A gravity current flows down the slope, exiting the sloping region beneath an apparently quiescent region 'I' and finally separating from the bottom boundary 'J'. Additionally we obtained velocity vector maps using a particle image velocimetry (PIV) method detailed in Stevens & Coates (1994). An example of such an image is given in figure 3, which corresponds with figure 2.

From the leading edge of the forcing plate (directly above the slope break-point, see figure 4) the turbulent boundary layer is unconstrained until it finally grows to meet the oppositely directed gravity current underflow down the slope, at which point the boundary layer thickness is h. This unconstrained portion of the boundary layer determines the discharge from the forcing region, as continuity requires that the boundary layer discharge be the same as the gravity current discharge down the underlying slope. From Sturman, Ivey & Taylor (1996) the discharge per unit width is:

$$Q \sim \left(B\ell_1\right)^{1/3} h, \qquad (1)$$

where

$$h \sim \ell_1. \qquad (2)$$

In the present case the geometry in the wedge gives the scale height over which the boundary layer discharges as:

$$h \sim \ell_1 \sim \ell \tan\theta/(1+\tan\theta). \qquad (3)$$

From (1), (2) and (3) the discharge for the wedge is given by

$$Q_{sc} \sim B^{1/3}\left(\ell \tan\theta/(1+\tan\theta)\right)^{4/3}, \qquad (4)$$

where θ is the angle of the bottom slope, B is the buoyancy flux out of the water surface and ℓ is the horizontal length of the forcing region over the slope.

Values of the dicharge from our experiments were calculated by integrating the vertical velocity profiles obtained from velocity vector maps like that in figure 3 and from others at the centre of the tank. We plot our non-dimensional experimental discharges in figure 5, in which we also present data drawn from a range of other laboratory, field and numerical experiments, ranging over three orders of magnitude of the discharge and with the angle of slope varying over approximately $0.4 \le \theta \le 22$ degrees.

The timescale of the flushing of the wedge is the ratio of the wedge volume to the discharge:

$$\tau_f \sim \ell^{2/3}(1+\tan\theta)^{4/3}/(B\tan\theta)^{1/3}. \qquad (5)$$

DISCUSSION AND CONCLUSION

The agreement of the data with the solid line representing the scaling in figure 5 is very good and the value of the coefficient for (4) is estimated to be 0.24 ($\rho^2 = 0.98$, where ρ is the correlation coefficient). The steady state discharge described by (4) shows a weak but necessary dependence upon the buoyancy flux. Discharge is more sensitive to angle of slope than to the forcing buoyancy flux. The results presented in this paper are readily applicable to studies of the exchange of nutrients and pollutants between littoral and pelagic zones of small water bodies where the Earth's rotation is of no consequence.

REFERENCES

Farrow, D.E. & Patterson, J.C. 1993 On the response of a reservoir sidearm to diurnal heating and cooling. *J. Fluid Mech.* **246** 143-161.

Horsch, G.M. & Stefan, H.G. 1988a Convective circulation in littoral water due to surface cooling. *Limnol. Oceanogr.* **33**, 1068-1083.

Horsch, G.M. & Stefan, H.G. 1988b *Cooling-induced convective littoral currents in lakes: simulation and analysis.* Project report no. 272, University of Minnesota St. Anthony Falls Hydraulic Laboratory.

Horsch, G.M., Stefan, H.G. & Gavali, 1994 Numerical simulation of cooling-induced convective currents on a littoral slope. *Intern. J. Num. Methods Fluids* **19**, 105-134.

James, W.F. & Barko, J.W. 1991 Estimation of phosphorus exchange between littoral and pelagic zone during nighttime convective circulation. *Limnol. Oceanogr.* **36**, 179-187.

Monismith, S., J. Imberger & M. L. Morison 1990 Convective motions in the sidearm of a small reservoir. *Limnology and Oceanography* **35**, 1676-1702.

Stevens, C. S. & Coates, M. J. 1994 A maximised cross-correlation technique for resolving velocity fields in laboratory experiments, *J. Hydr. Res.* **32**, 195-211.

Sturman, J.J., Ivey, G.N. & Taylor, J.R. 1996 Convection in a long box driven by heating and cooling on the horizontal boundaries. *J. Fluid Mech.* **310**, 61-87.

Sturman, J. J. & Ivey, G. N. 1998 Unsteady convective exchange flows in cavities. *J. Fluid Mech.* **368**, 127-153.

ACKNOWLEDGEMENTS: The authors thank S. Bell who helped with collection and processing of field data. This work was funded by the Australian Research council. Centre for Water Research Reference ED-1311-JS.

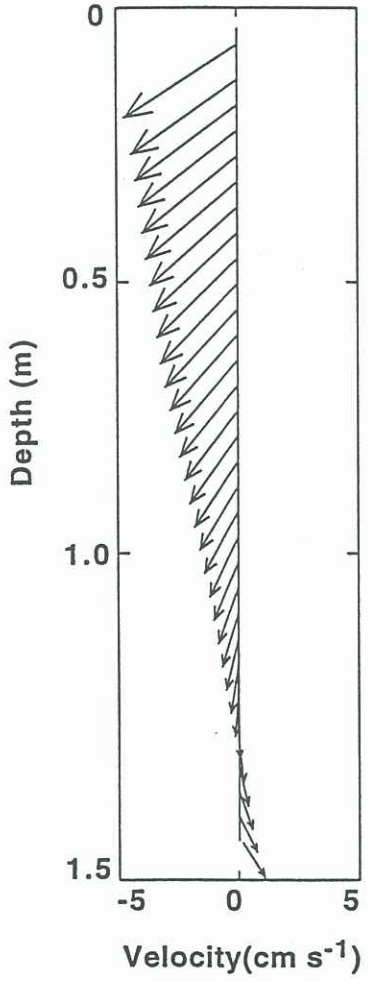

Figure 1 : 'Perspective' velocity profile of the resultant of the two horizontal velocity components collected near the end of the slope from the shore at 9:50 on day 248. The profile shows a reversal of velocities from top to bottom waters, which, when coincident with low wind speeds, is considered indicative of convective circulation.

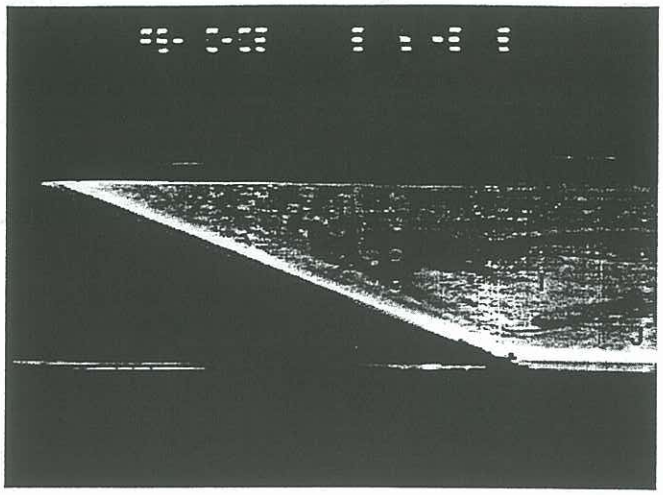

Figure 2 : Flow visualization of steady state wedge flow forced destabilizingly above the slope.

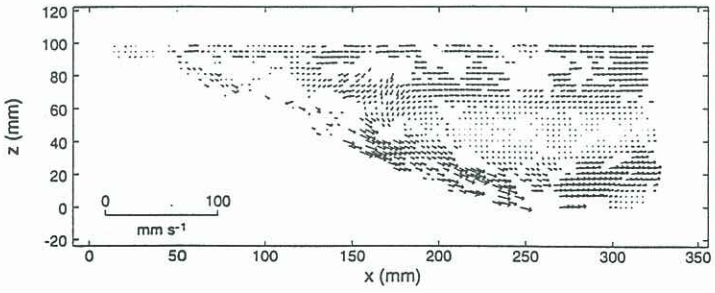

Figure 3 : This velocity vector map corresponds with figure 2. It derives from a PIV process and demonstrates intense flow down the slope with a maximum velocity of 18 mm s^{-1} in this case.

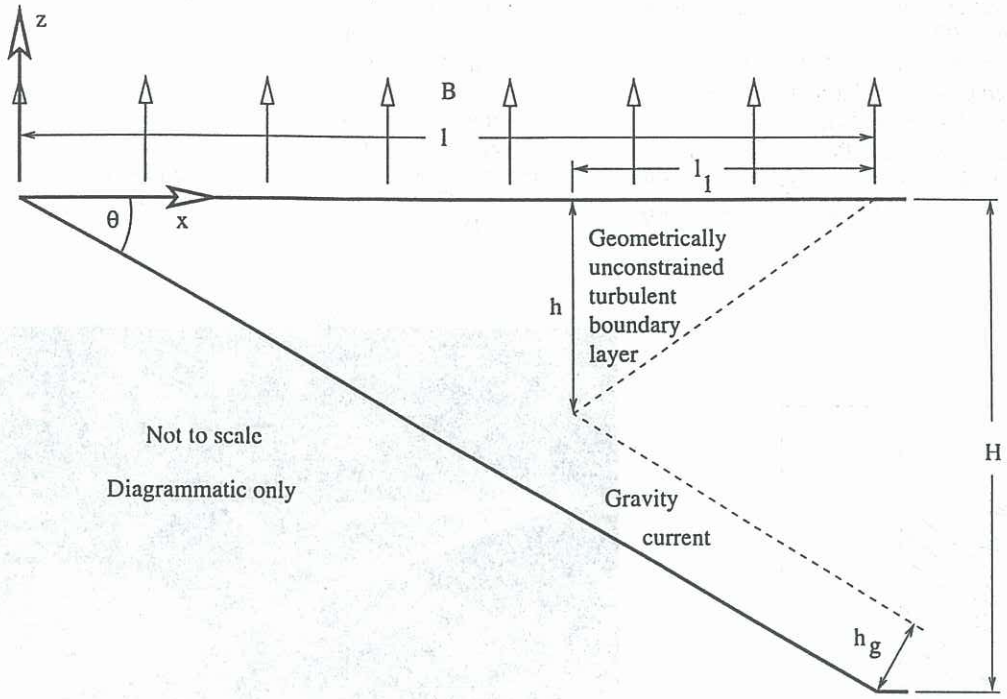

Figure 4 : Definition of axes and major symbols in the sloping region.

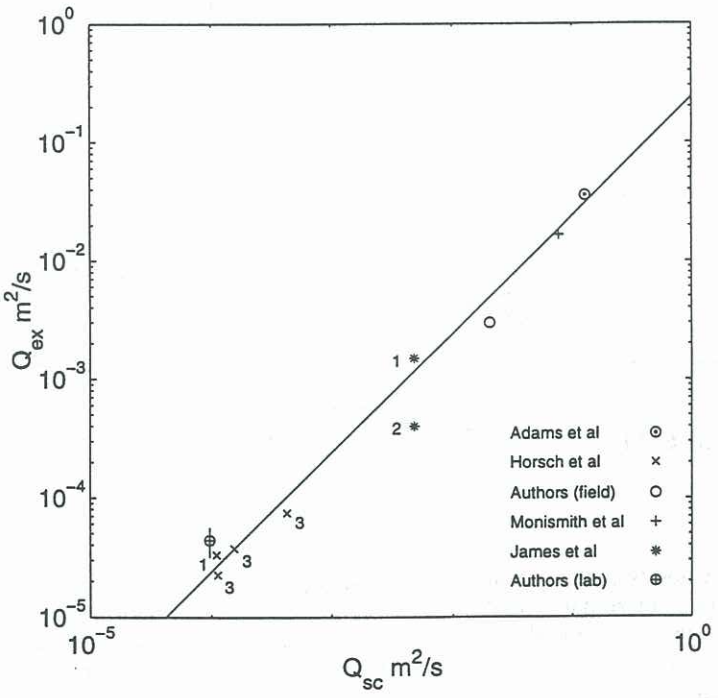

Figure 5 : Plot of discharge predicted by scaling (solid line, equation (4) with a coefficient of 0.24) against forcing flux for a range of laboratory, field and numerical experiments.